Performance Analysis of Three-Phase Shunt Active Power Filter for Harmonic Mitigation

Samson Dauda Yusuf [a*], Abdulmumini Zubairu Loko [a] and Jibrin Abdullahi [b]

[a] *Department of Physic, Faculty of Natural and Applied Sciences, Nasarawa State University, Keffi, Nigeria.*
[b] *Department of Electrical/Electronic Engineering Technology, School of Engineering Technology, Isa Mustapha Agwai I Polytechnic Lafia, Nasarawa State, Nigeria.*

Authors' contributions

This work was carried out in collaboration among all authors. All authors contributed to the study conception and design. Material preparation, data collection and analysis were performed by authors SDY, AZL and JA. The first draft of the manuscript was written by author SDY, reviewed and re-drafted by author SDY, and all authors commented on previous versions of the manuscript. All authors read and approved the final manuscript.

Original Research Article

ABSTRACT

Aims: To carried out performance analysis of a shunt active power filter (SAPF) for harmonics mitigation.
Study Design: Experimental design through simulation studies using P-Q Theory and proportional integral controller.
Place and Duration of Study: Department of Physics, Nasarawa State University Keffi, main campus, Nigeria, between October 2020 and September 2021.
Methodology: Primary and secondary data were obtained using AVO Digital Multimeter and manufacturers' datasheets from Schneider electric website to capture required system parameters, SAPF was designed using a Voltage Source Inverter model to represent the Three-Phase source, and P-Q Theory with PI Control was used for reference current extraction. The SAPF was modeled, designed and simulated using MATLAB-Simulink and analyzed under different nonlinear load conditions and harmonic spectrum to achieve low Total Harmonic Distortion (THD).
Results: The THD in the unbalanced system voltages before the application of SAPF was found to be 12.6%, 11.4% and 11.2%, while after the application of SAPF was 2.2%, 2.5% and 2.5% for phase voltages a, b and c respectively. The grid currents indicated THD of 27.2%, 30.9% and 31%

_____

Corresponding author: E-mail: samsonyusufu@yahoo.com, samson720@snu.ac.kr;

before application of SAPF and 2.2%, 2.2% and 2.1% after application.

Conclusion: The use of non-linear loads; has adverse effects on the quality of electric power as well as phase voltage and frequency waveforms. The use of SAPF is of vital importance in improving electric power quality for reliable power supply and quality service delivery.

1. INTRODUCTION

"Electrical loads, drawing sinusoidal current from a sinusoidal voltage source, are called linear loads. They consist of only resistive (R), inductive (L) and capacitive (C) passive elements" [1]. "Non-linear loads draw non-sinusoidal current waveform, although they are fed from a sinusoidal voltage source. These nonlinear loads control the flow of power by drawing currents only during certain intervals of the 50/60 Hz period. Thus, the current drawn by the nonlinear load is non-sinusoidal and appears chopped or flattened" [2]. The increasing use of power electronics based non-linear loads; has adverse effects on the quality of electric power, thereby impeding the maintenance of purely sinusoidal current waveform as well as phase voltage and frequency waveforms [3]. "Therefore, a power quality problem occurs if any of the voltage, current or frequency deviation from sinusoidal nature. Power quality problems are common in developing economies especially in Nigeria, in the areas of industrial, commercial and utility networks; as power electronics appliances are used more in these fields. These appliances generate harmonics and reactive power" [4].

According to IEEE Standard 519, "A sinusoidal component of a periodic wave or quantity having a frequency that is an integral multiple of the fundamental frequency is defined as harmonic" [5]. "Any periodic, distorted waveform can be expressed as a sum of pure sinusoids. The sum of sinusoids is referred to a Fourier series, which permits a periodic distorted waveform to be decomposed into an infinite series containing DC component, fundamental component (50/60 Hz for power systems) and its integer multiples called the harmonic components. The harmonic number (h) usually specifies a harmonic component, which is the ratio of its frequency to the fundamental frequency" [6]. "Harmonic distortion can have detrimental effects on electrical distribution systems; waste energy and lower the capacity of an electrical system and also harm the devices operating on the system.

Therefore, understanding the problems associated with harmonic distortion, its causes and effects, as well as the methods of dealing with it, is of great importance in minimizing those effects and increasing the overall efficiency of the distribution system" [4]. "Therefore it is very important to compensate the dominant harmonics and thus Total Harmonic Distortion (THD) below 5% as specified in IEEE 519 harmonic standard" [7].

"The passive filtering is the simplest solution to eliminate the harmonic distortion and power factor improvement in the power system utilities. However, passive filter suffer from many disadvantages such as tuning problems due to tolerance, resonance, fixed compensation characteristics for fixed value of L & C and their bulky size" [8]. "The Active Power Filter (APF) technology has been in use for providing compensation for harmonics, reactive power, and/or neutral current in ac networks. It has evolved in the past quarter century of development with varying configurations, control strategies, and solid-state devices" [9]. "APF's are also used to eliminate voltage harmonics, to regulate terminal voltage, to suppress voltage flicker, and to improve voltage balance in three-phase systems. This wide range of objectives is achieved either individually or in combination, depending upon the requirements and control strategy and configuration which have to be selected appropriately" [10]. "Starting in 1971, many configurations, such as the active series filter, the active shunt filter and the combination of the shunt and the series filter have been developed and commercialized also for uninterruptible power supply (UPS) applications" [11]. The shunt active power filter is the simplest configuration, as well as the most commonly employed owing to its vast application in compensation for nonlinear loads, parallel injection of the harmonic components of the load current, as well as better compensation of the reactive components, and the unbalance components at the fundamental frequency [12]. In view of the above, the main objective of this study is to design and simulate a three-phase

shunt active power filter which is a dynamic and flexible solution for the mitigation of harmonic current due to their compact size, no requirement of tuning and stable operation. The study will provide valuable support material for industry players in improving electric power quality for both utility and consumers through mitigation of harmonics components in the system power signals.

2. MATERIALS AND METHODS

2.1 Materials

The materials that were used in this study includes AVO 830 Advanced Multimeter for measuring the grid quantities, laptop, and MATLAB software Version R2014b for designing the SAPF, modelling and simulation, and. Secondary data in form of manufacturers' datasheets obtained from Schneider Electric website.

2.2 Methods

2.2.1 SAPF simulation method

Primary data was collected over a period of 365 days, using AVO Digital Multimeter to capture system voltage and AC resistive, inductive and capacitive (RLC) components, as well as transient system parameters for processing and analysis. Secondary data in form of manufacturers' datasheets was also obtained from Schneider Electric website. Traditional calculations; as well as modeling and simulation using MATLAB version R2014b were utilized for the data analysis. Mathematical/functional blocks were developed in Simulink and then parameterized using the designed parameters in the available Simulink parameter blocks; after which the designed models were simulated.

2.2.2 SAPF design method

The design and simulation of the SAPF was carried out in MATLAB Version R2014b using information on the nature of the load (harmonic source), i.e. whether 3-phase or 1-phase; the harmonic current extraction method; and the type of control scheme. The proposed study was carried out using a three phase harmonic source using the generalized P-Q current extraction method with simple Proportional Integral (PI) Controller. The shunt connected VSI based SAF, with a self-controlled DC bus (capacitor on the DC side) has a topology similar to that of static compensator (STATCOM) used for reactive power compensation. The SAF injects a harmonic signal with the same amplitude as that of the load into the ac system but with opposite phase displacement enabling it to operates as a current source, injecting the harmonic component generated by the load but with a phase-shifted of 180˚. The block diagram of the proposed system is shown in Fig. 1.
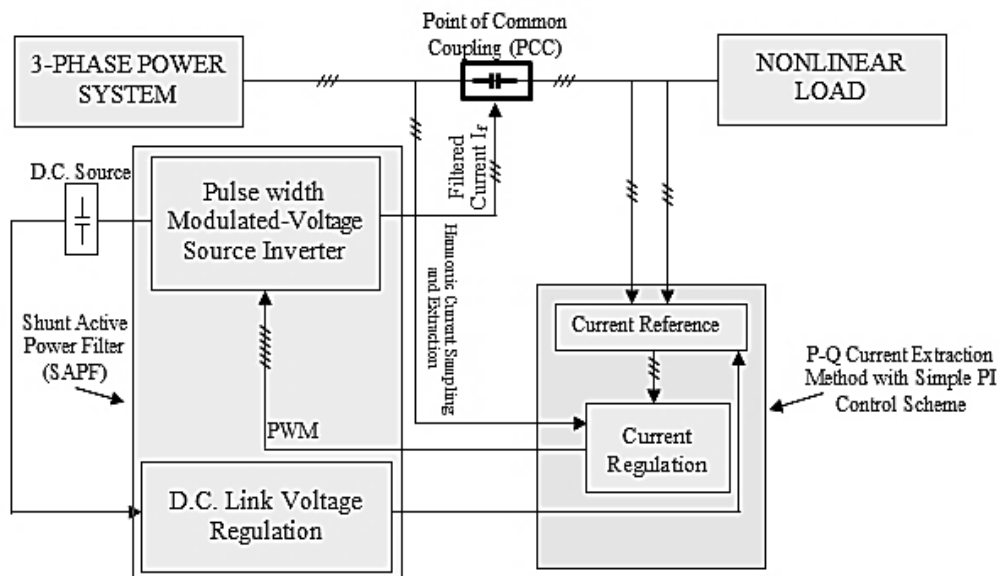

Fig. 1. Block Diagram of the Shunt Active Power Filter

2.2.2.1 Harmonic currents extraction method

This current extraction method uses the transformation of distorted currents from three phase frame *abc* into bi-phase stationary frame *αβ*. The basic idea is that the harmonic currents caused by nonlinear loads in the power system can be compensated with other nonlinear controlled loads. The p-q theory is based on a set of instantaneous powers defined in the time domain. The three-phase supply voltages (*ua, ub, uc*) and currents (*ia, ib, ic*) are transformed using the Clarke (or α-β) transformation yielding instantaneous active and reactive power components. The Clarke transformation for the voltage variables as defined by Akagi et al. [13] is given by:

$$\begin{bmatrix} u_\alpha \\ u_\beta \\ u_0 \end{bmatrix} = \frac{\sqrt{2}}{3} \begin{bmatrix} 1 & -\frac{1}{2} & -\frac{1}{2} \\ 0 & \frac{\sqrt{3}}{2} & -\frac{\sqrt{3}}{2} \\ \frac{1}{\sqrt{2}} & \frac{1}{\sqrt{2}} & \frac{1}{\sqrt{2}} \end{bmatrix} \begin{bmatrix} u_a \\ u_b \\ u_c \end{bmatrix} \tag{1}$$

Similarly, this transform can be applied on the distorted load currents to give:

$$\begin{bmatrix} i_{I\alpha} \\ i_{I\beta} \\ i_{I0} \end{bmatrix} = \frac{\sqrt{2}}{3} \begin{bmatrix} 1 & -\frac{1}{2} & -\frac{1}{2} \\ 0 & \frac{\sqrt{3}}{2} & -\frac{\sqrt{3}}{2} \\ \frac{1}{\sqrt{2}} & \frac{1}{\sqrt{2}} & \frac{1}{\sqrt{2}} \end{bmatrix} \begin{bmatrix} i_a \\ i_b \\ i_c \end{bmatrix} \tag{2}$$

Akagi et al. [13] further represented the instantaneous active power *p(t)* as:

$$p(t) = u_a i_{Ia} + u_b i_{Ib} + u_c i_{Ic} \tag{3}$$

This expression can be given in the stationary frame by:

$$\begin{cases} p(t) = u_\alpha i_{I\alpha} + u_\beta i_{I\beta} \\ p_0(t) = u_0 i_{I0} \end{cases} \tag{4}$$

Where, *p(t)* is the instantaneous active power, P_o *(t)* is the instantaneous homo-polar sequence power. Similarly the instantaneous reactive power as defined by Akagi et al. [13] can be given by:

$$q(t) = -\frac{1}{\sqrt{3}}[(u_a - u_b)i_{Ic} + (u_b - u_c)i_{Ia} +$$
$$uc-uail b = uai l\beta - u\beta il\alpha \tag{5}$$

Note: The instantaneous reactive power takes in consideration all the current and voltage harmonics, whereas the habitual reactive power

considers just the fundamentals of current and voltage. From eqns. 4 and 5 the instantaneous active and reactive power can be given in matrix form by:

$$\begin{bmatrix} p \\ q \end{bmatrix} = \begin{bmatrix} u_\alpha & u_\beta \\ u_\beta & u_\alpha \end{bmatrix} \begin{bmatrix} i_{I\alpha} \\ i_{I\beta} \end{bmatrix} \tag{6}$$

Note: Each one of the active and reactive instantaneous powers contains a direct component which presents the power of the fundamentals of current and voltage and an alternating component which presents the power of the harmonics of currents and voltages. To separate the harmonics from the fundamentals of the load currents, it is enough to separate the direct term of the instantaneous power from the alternating one. Here, a Low Pass Filter (LPF) with feed-forward effect can be used to accomplish this task. Hence, the harmonic components of the load currents can be given using the inverse of equation (6) as explained by Singh et al. [14] as:

$$\begin{bmatrix} i_{I\alpha} \\ i_{I\beta} \end{bmatrix} = \frac{1}{v_{s\alpha}^2 + v_{s\beta}^2} \begin{bmatrix} v_{s\alpha} & -v_{s\beta} \\ v_{s\beta} & v_{s\alpha} \end{bmatrix} \begin{bmatrix} \tilde{p}_I \\ \tilde{q}_I \end{bmatrix} \tag{7}$$

The APF reference current can be then given by equation (8) as follows:

$$\begin{bmatrix} i_{fa}^* \\ i_{fb}^* \\ i_{fc}^* \end{bmatrix} = \frac{\sqrt{2}}{2} \begin{bmatrix} 1 & 0 \\ -\frac{1}{2} & \frac{\sqrt{3}}{2} \\ -\frac{1}{2} & -\frac{\sqrt{3}}{2} \end{bmatrix} \begin{bmatrix} \tilde{\imath}_{I\alpha} \\ \tilde{\imath}_{I\beta} \end{bmatrix} \tag{8}$$

The principle of the active and reactive instantaneous power is shown in Fig. 2.

2.2.2.2 Voltage source inverter

Because of its lower THD in output signals, the 3-phase, 2-level voltage source inverter (VSI) is adopted for the purpose of this study. It is composed of three-legs with current reversible switches, realized by controlled switches (GTO or IGBT) with anti-parallel diodes to allow the flow of the free-wheeling currents as shown in Fig. 3. Here, the switches of any leg of the inverter (T1 and T4, T2 and T5, T3 and T6) cannot be switched ON simultaneously because this would result in a short circuit across the dc link voltage supply. Similar to this, switching off all switches on one leg of the inverter at once will cause voltages that rely on the polarity of the respective line current, which will lead to undefined states in the VSI and undefined ac output line voltages.
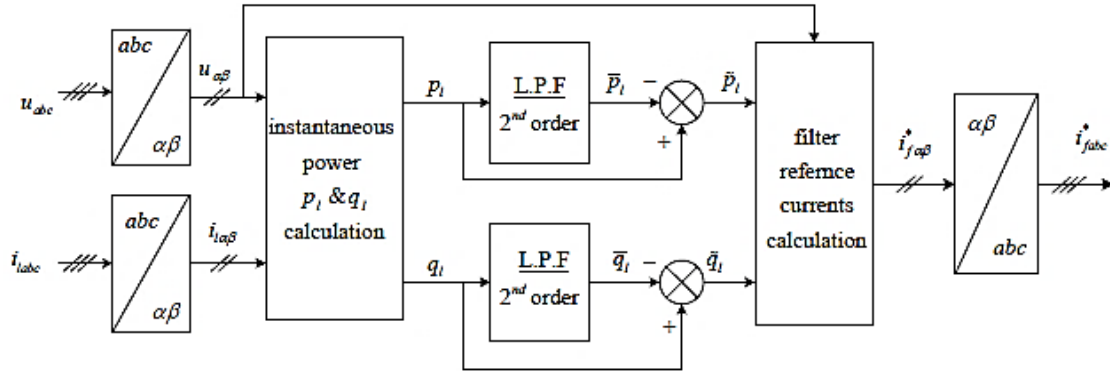
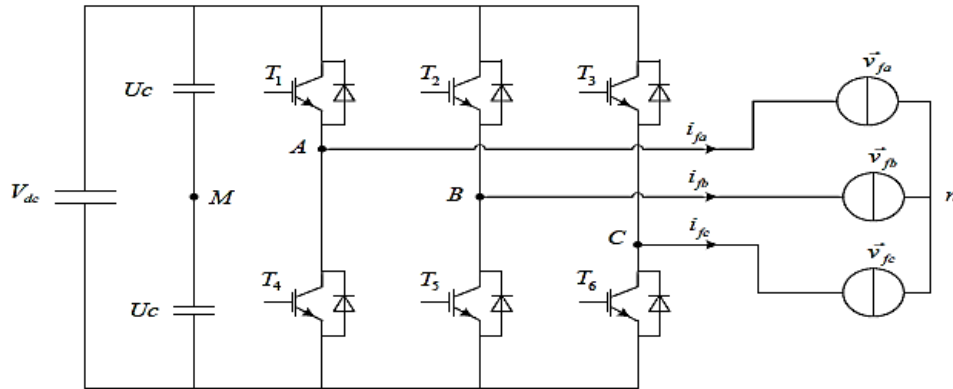**Fig. 2. Principle of Instantaneous Active and Reactive Power Theory [14]**

Fig. 3. The voltage source inverter (3-phase, 2-level topology used) [8]

2.2.2.3 Modeling of the voltage source inverter

The output of the VSI which is shown in Fig. 3 can take two levels of voltage (+Vdc, - Vdc) depending on the dc source voltage and the switches states. Actually, the control of the two switches on the same leg is complementary: the conduction of one of them implies the blocking of the other. The SAPF Model showing its connection at the Point of Common Coupling (PCC) is shown in Fig.4, where the voltages of the points A, B, and C to the imaginary point M can be given by:

$$\begin{cases} V_{AM} = U_C \cdot (2S_a - 1) \\ V_{BM} = U_C \cdot (2S_b - 1), with\ U_c = \frac{V_{dc}}{2} \\ V_{CM} = U_C \cdot (2S_c - 1) \end{cases} \quad (9)$$

The simplified voltages of the VSI can then be given by:

$$\begin{cases} v_{fa} = V_{An} = 2U_C \frac{2S_a - S_b - S_c}{3} = V_{dc} \frac{2S_a - S_b - S_c}{3} \\ v_{fb} = V_{Bn} = 2U_C \frac{2S_b - S_a - S_c}{3} = V_{dc} \frac{2S_b - S_a - S_c}{3} \\ v_{fc} = V_{Cn} = 2U_C \frac{2S_c - S_b - S_a}{3} = V_{dc} \frac{2S_c - S_b - S_a}{3} \end{cases} \quad (10)$$

The eight valid switch states are given in Table 1 as follows:

Table 1. Valid Switch States for the VSI

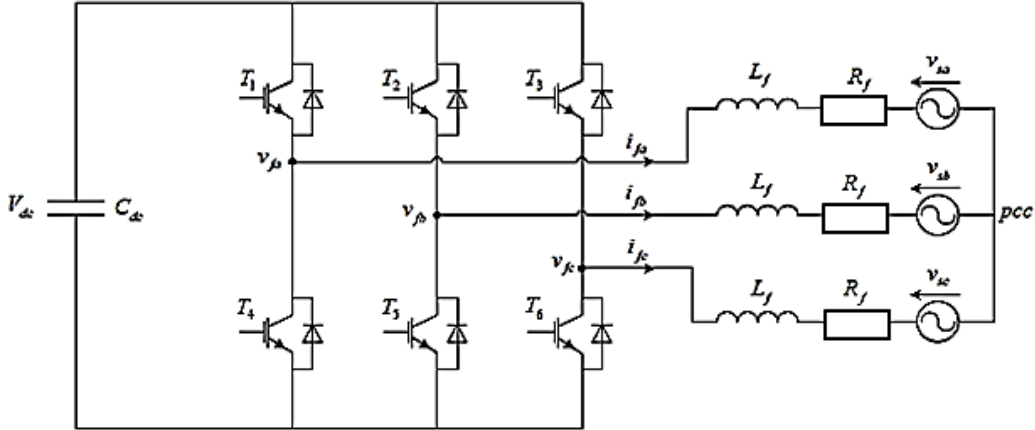| State	S_a	S_b	S_c	Vf$_a$	Vf$_b$	Vf$_c$	α+jβ
0	0	0	0	0	0	0	0+j0
1	1	0	0	2/3	-1/3	-1/3	0,8+j0
2	0	1	0	-1/3	2/3	-1/3	-0.4+j0.7
3	1	1	0	1/3	1/3	-2/3	0.4+j0.7
4	0	0	1	-1/3	-1/3	2/3	-0.4-j0.7
5	1	0	1	1/3	-2/3	1/3	0.4-j0.7
6	0	1	1	-2/3	1/3	1/3	-0.81+j0
7	1	1	1	0	0	0	0+j0

Fig. 4. The SAPF Model showing the Point of Common Coupling (PCC) [8]

The VSI control technique based on the Sinusoidal Pulse Width Modulation (SPWM) is adopted in this study owing to its ability to stabilize its switching frequency. It uses a fixed switching frequency of 20 kHz, which makes it easier to cancel the switching harmonics. SPWM determines the voltage reference of the inverter from the error between the measured current and its reference. This reference voltage is then compared with a triangular carrier signal (with high switching frequency).

2.2.2.4 Modeling of the active power filter

The connection of the shunt active power filter to the point of common coupling of the grid is done mostly by the means of a RL low pass filter as shown in Fig. 4. The voltage equation for each phase as reported by Chauhan et al. [15] can be given by:

$$v_{sk} = v_{fk} - v_{L_{fk}} - v_{R_{fk}} = v_{fk} - L_f \frac{di_{fk}}{dt} - R_f i_{fk}, k = a, b, c \tag{11}$$

The three phase equations are then given by:

$$L_f \frac{d}{dt} \begin{bmatrix} i_{fa} \\ i_{fb} \\ i_{fc} \end{bmatrix} = -R_f \begin{bmatrix} i_{fa} \\ i_{fb} \\ i_{fc} \end{bmatrix} + \begin{bmatrix} v_{fa} \\ v_{fb} \\ v_{fc} \end{bmatrix} - \begin{bmatrix} v_{sa} \\ v_{sb} \\ v_{sc} \end{bmatrix} \tag{12}$$

And for the dc side; Chauhan et al. [15] defined this as:

$$C_{dc} \frac{dV_{dc}}{dt} = S_a i_{fa} + S_b i_{fb} + S_c i_{fc} \tag{13}$$

The equation system defining the SAPF in the three phase frame is then given by:

$$\begin{cases} L_f \frac{di_{fa}}{dt} = -R_f i_{fa} + v_{fa} - v_{sa} \\ L_f \frac{di_{fa}}{dt} = -R_f i_{fb} + v_{fb} - v_{sb} \\ L_f \frac{di_{fa}}{dt} = -R_f i_{fc} + v_{fc} - v_{sc} \\ C_{dc} \frac{dV_{dc}}{dt} = S_a i_{fa} + S_b i_{fb} + S_c i_{fc} \end{cases} \tag{14}$$

2.2.2.5 Sinusoidal Pulse Width Modulation (SPWM) control

PWM can be implemented using a variety of methods, including space vector PWM, PWM with harmonics minimization, and carrier-based PWM. Natural PWM, symmetric PWM, and asymmetric PWM are all possible for the carrier PWM. A controller is used, which determines the voltage reference of the inverter from the error between the measured current and its reference. This reference voltage is then compared with a triangular carrier signal (with high switching frequency). The output of this comparison gives the switching function of the VSI as shown in Fig. 5. The choice of the ratio between the frequency of the reference signal and that of the carrier signal is very important in case of symmetrical and periodic reference. In the case of sinusoidal reference, the ratio between the two frequencies must be an integer in order to synchronize the carrier signal with the reference signal. In both situations, it must be high enough to ensure quick switching and reduce switching harmonics in the inverter's fundamental output. In order to preserve the reference symmetry, it is also ideal for the carrier frequency to be odd.

2.2.2.6 Control method of the active power filter

The indirect control method of SAPF was adopted in this study owing to its less

complicated, but highly effective control algorithm and fewer sensors are needed than in the direct control method. The method is based on the measurement of the source currents, and then imposing the sinusoidal form on these currents. Fig.6 shows the indirect control method of the SAPF. Here, the objective is in the control of the grid currents without looking at the filter currents. Sinusoidal current reference for the grid is generated using appropriate method (Instantaneous P-Q Theory). These currents are then compared with the measured grid currents. The error is fed to a hysteresis current controller which generates the pulses to control the switches of the SAPF. The P-Q theory offers very effective and flexible alternative for compensation of frequency and reactive power, which are the most prevalent power quality issues in the modeled (Nigerian) grid system, hence its adoption in this study. The indirect control method of the SAPF is shown in Fig. 6.

2.2.2.7 Grid current generation method using PQ theory based algorithm

Unlike the direct method; which uses both instantaneous active and reactive powers when adopting the P-Q Theory-based algorithm, the indirect method uses just the instantaneous active power, as such, the alternative components of the instantaneous active power are eliminated. The direct components are then used to generate grid currents. The reactive power is imposed to be zero to allow the compensation of the current harmonics and the reactive power at the same time. In three phase system without neutral, the simple voltages of the PCC v_{sa}, v_{sb}, v_{sc} and the load currents i_{La}, i_{Lb}, i_{Lc} are given in the stationary frame reference by:

$$\begin{bmatrix} \hat{v}_{s\alpha} \\ \hat{v}_{s\beta} \end{bmatrix} = \frac{\sqrt{2}}{3} \begin{bmatrix} 1 & -\frac{1}{2} & -\frac{1}{2} \\ 0 & \frac{\sqrt{3}}{2} & -\frac{\sqrt{3}}{2} \end{bmatrix} \begin{bmatrix} \hat{v}_{sa} \\ \hat{v}_{sb} \\ \hat{v}_{sc} \end{bmatrix} \qquad (15)$$
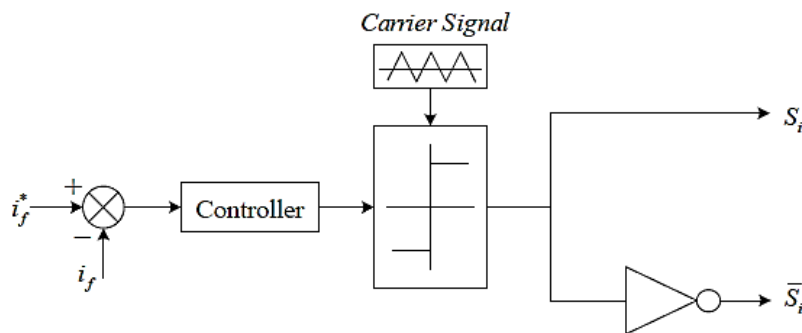

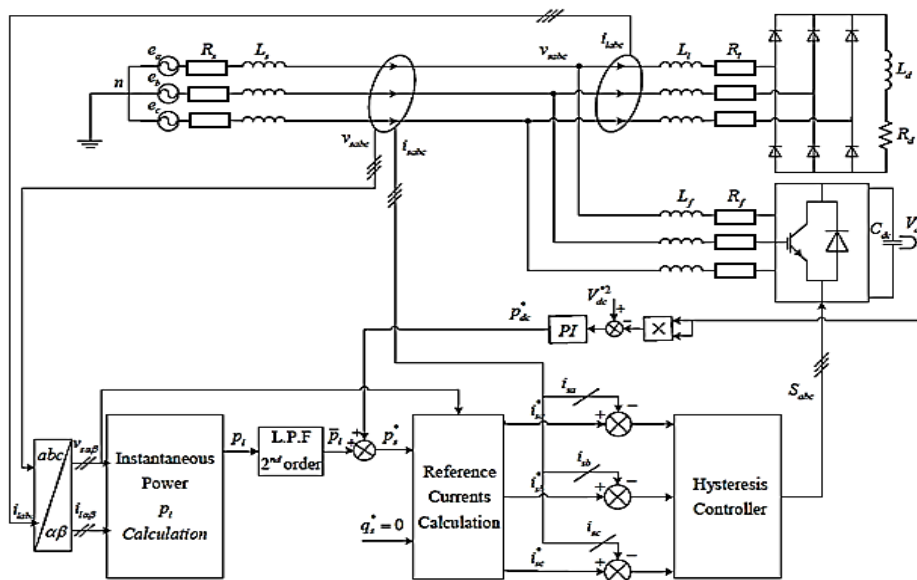**Fig. 5. The Sinusoidal PWM Control Method for the VSI [14]**

Fig. 6. Indirect control of SAPF based on the instantaneous power theory [14]

$$\begin{bmatrix} i_{I\alpha} \\ i_{I\beta} \end{bmatrix} = \frac{\sqrt{2}}{3}\begin{bmatrix} 1 & -\frac{1}{2} & -\frac{1}{2} \\ 0 & \frac{\sqrt{3}}{2} & -\frac{\sqrt{3}}{2} \end{bmatrix}\begin{bmatrix} i_{Ia} \\ i_{Ib} \\ i_{Ic} \end{bmatrix} \tag{16}$$

Neglecting the voltage harmonics, the instantaneous active power is given by:

$$P_I = v_{s\alpha}i_{I\alpha} + v_{s\beta}i_{I\beta} \tag{17}$$

This active power can be decomposed into two components, the first direct representing the power of the fundamentals of the voltage and current. The second component is alternative due to the harmonics of the current and voltage.

$$P_I = \bar{P}_I + \tilde{P}_I \tag{18}$$

The reference power on the source side is given by:

$$P_I^* = \bar{P}_I + P_{dc}^* \tag{19}$$

Where: P_{dc}^* is the amount of power used to compensate the losses in the filter and to keep its voltage constant. This term is generated using the direct voltage controller. The direct component of the active power can be extracted using low pass filter of the second or third order to filter the instantaneous active power. The reference currents of the grid are then given by:

$$i_{s\alpha}^* = \frac{v_{s\alpha}}{v_{s\alpha}^2+v_{s\beta}^2}P_s^* \tag{20}$$

$$i_{s\beta}^* = \frac{v_{s\beta}}{v_{s\alpha}^2+v_{s\beta}^2}P_s^* \tag{21}$$

The reference currents in the three phase frame are then given by:

$$\begin{bmatrix} i_{sa}^* \\ i_{sb}^* \\ i_{sc}^* \end{bmatrix} = \frac{\sqrt{2}}{3}\begin{bmatrix} 1 & 0 \\ -\frac{1}{2} & \frac{\sqrt{3}}{2} \\ -\frac{1}{2} & -\frac{\sqrt{3}}{2} \end{bmatrix}\begin{bmatrix} \tilde{i}_{I\alpha} \\ \tilde{i}_{I\beta} \end{bmatrix} \tag{22}$$

2.2.2.8 Design of PI controller for the indirect control method

As suggested by Balasubramania and Palani [16], the input of the PI controller is the error between the stored energy in the capacitor and its reference value. Its output represents the reference power of the three-phase system at the PCC defined by:

$$P_s^* = \frac{3V_{s\_peak}i_{s\_peak}}{2} \tag{23}$$

The reference power of the filter represents the difference between the grid reference power and the load power, supposing that the filter is able to produce its reference power in each period. This power P_f^* represents the transmitted power from the source to the filter, neglecting the losses of the filter and the coupling inductance. The integral of the filter power gives the energy stored in the condenser. Fig. 7 shows the diagram of the voltage regulation.
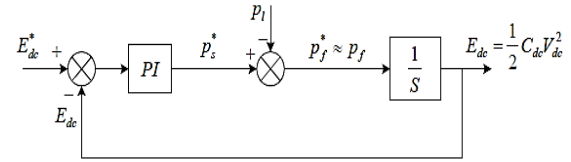

Fig. 7. DC Voltage Closed Loop Control

From Fig. 7, the stored energy of the condenser can be defined as:

$$P_s^* = G_{PI}(S)\left(E_{C_{dc}}^* - E_{C_{dc}}\right) \tag{24}$$

$$E_{C_{dc}} = (P_s^* - P_I)\frac{1}{S} \tag{25}$$

By substituting Equation 24 in 25, we get:

$$E_{C_{dc}} = \frac{G_{PI}(S)}{S+G_{PI}(S)}E_{C_{dc}}^* - \frac{1}{S+G_{PI}(S)} \tag{26}$$

where G_{PI} is the transfer function of the PI controller defined by:

$$G_{PI}(S) = k_{p\_dc} + \frac{k_{i\_dc}}{S} \tag{27}$$

By substituting the transfer function equation 27 in equation 26, the closed loop transfer function of the system can be given by:

$$E_{C_c} = \frac{k_{p\_dc}S+k_{i\_dc}}{S^2+k_{p\_dc}S+k_{i\_dc}}E_{C_{dc}}^* - \frac{S}{S^2+k_{p\_dc}S+k_{i\_dc}}P_I \tag{28}$$

Comparing this transfer function with the canonic form of a second order transfer function we find:

$$\begin{cases} k_{p\_dc} = 2\xi\omega_{cdc} \\ k_{i\_dc} = \omega_{cdc}^2 \end{cases} \tag{29}$$

where optimum value of ξ = 0.707 is the damping factor. The cut-off frequency *fc = 8* Hz was chosen.

2.2.2.9 Design parameters of shunt active filter

As mentioned earlier, a three-leg voltage source converter (VSC) is used to model the active filter

and it has six insulated-gate bipolar transistors (IGBTs), three interface inductors, and one dc capacitor. The line to line voltage (V_{L-L}) of the VSC is considered as 415V. The AC inductor and the DC capacitor selection are described as follows.

DC Capacitor Voltage: The minimum dc bus voltage should be greater than twice the peak value of the system phase voltage given as:

$$V_{dc} = \frac{2\sqrt{2}V_{L-L}}{(\sqrt{3}m)} \qquad (30)$$

Where, m is the modulation index and is considered as 1.

DC Bus Capacitor: The value of dc capacitor (C_{dc}) depends on the instantaneous energy available to the active filter during transients. Using the principle of energy conservation, we have:

$$\frac{1}{2}C_{dc}[(V_{dc}^2) - (V_{dc1}^2)] = 3V(aI)t \qquad (31)$$

Where, V_{dc} is the reference dc voltage and V_{dc1} is the minimum voltage level of dc bus, '*a*' is the overloading factor, V is the phase voltage, I is the phase current and 't' is time taken for the dc bus voltage to be recovered.

AC Inductor: The selection of the ac inductance (L_f) depends on the current ripple $i_{cr(p-p)} = 5\%$, switching frequency f_s, dc bus voltage (V_{dc}) and the overloading factor given as:

$$L_f = \frac{(\sqrt{3}mV_{dc})}{12af_s i_{cr(p-p)}} \qquad (32)$$

Where 'm' is the modulation index; and 'a' is the overload factor.

2.2.2.10 Measurement of total harmonic distortion

The Total Harmonic Distortion (THD) of the system was determined using the obtained rms values of the voltages and currents at the given fundamental frequency as well as those voltages and currents measured at all of the selected harmonic levels (3rd, 5th, 7th and 9th harmonics). The SAF was used to split the signal into two parts: a signal with all of the harmonics filtered out leaving just the fundamental frequency, and a signal with the fundamental frequency filtered out leaving all of the harmonics. Then the rms value of each of those two parts was measured; the

following the works of Aher et al. [10], the THD was calculated as follows:

$$THD = \frac{\sqrt{\sum_{n=2}^{\infty} V_{n\_rms}^2}}{V_{fund\_rms}} \times 100\% \qquad (33)$$

3. RESULTS

3.1 Data Specifications

The measured system parameters used in modeling the SAPF are presented in Table 2. The simulated system is a three phase balanced and non-balanced voltage system, which is represented by a voltage source inverter with the non-linear load modeled as a three phase non controlled bridge rectifier.

The data in Table 2 are tabulated from two different collections; namely the SAPF parameters obtained from the manufactures' datasheet information and the system parameters measured using the advanced digital AVO meter. The first six (6) parameters were measured from the grid supply using the advanced digital AVO. The next four parameters were obtained from the SAPF datasheet information from the manufacturers' (Schneider Electric) website; while the last four (4) parameters represent the synthetic loads imposed on the SAPF in order to study its dynamic response.

3.2 Design and Modeling of the System

The system model was built in MATLAB/Simulink and the simulation results of the performance of SAPF in the compensation of system harmonics in the three phase unbalanced grid are presented. A linear inductive load is connected in parallel with the non-linear load. The analytical behavior of Shunt Active Filter with the three-phase source and shunt active power filter were connected in parallel to the distribution linear and non-linear load.

3.2.1 DC voltage source and regulator control

The DC source for the VSI is a simulated 3-phase source whose signal is provided through DC voltage regulation using a dc link capacitor. 3-phase model is also developed within the MATLAB environment as shown in Fig. 8.In the simple PI control scheme, the peak value of the reference grid current I*peak is determined by the DC voltage regulator. The unit vectors of voltage at the PCC are simply multiplied by the peak value of the grid current to produce the reference currents for the grid.

Table 2. Designed parameters of the system

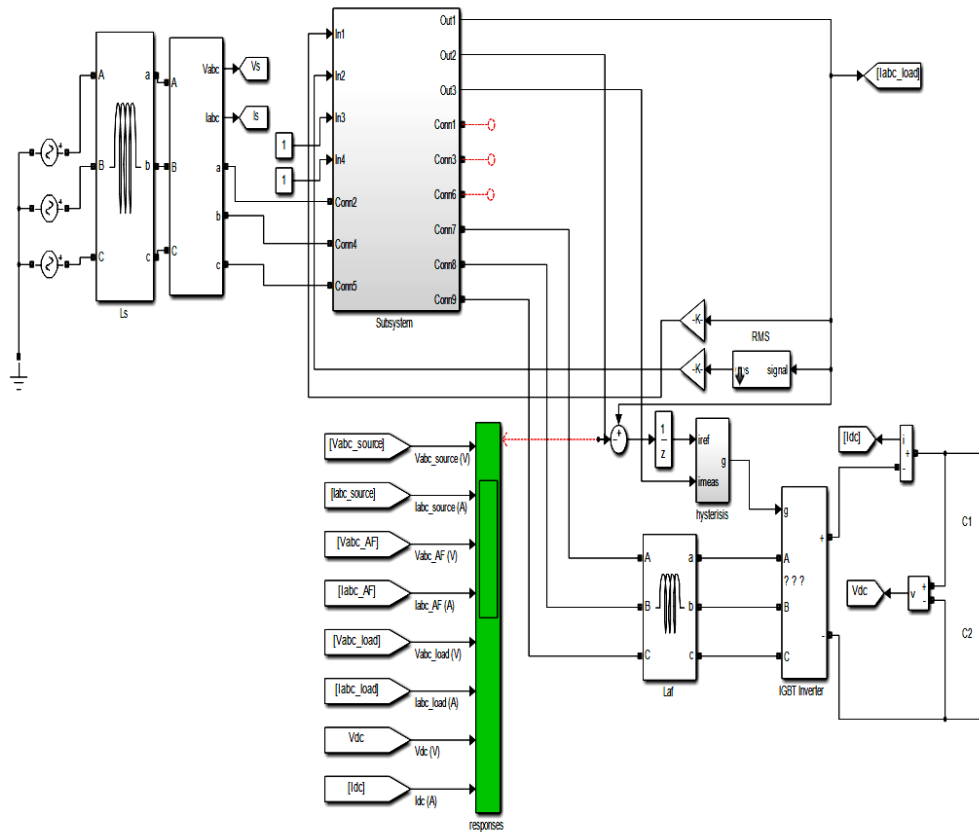| Symbol	Quantity	Value
V_s	Ideal grid voltage L-L	415V
f	Grid frequency	50Hz
R_s	Grid resistance	3mΩ
L_s	Grid inductance	2.6µH
R_L	AC load resistance	10mΩ
L_L	AC load inductance	0.3mH
R_f	Filter resistor	20mΩ
L_f	Filter inductance	0.2mH
C_{dc}	APF DC capacitor	5 mF
V_{dc}	DC link capacitor	900 V
$Load\ 1$	DC Load Resistance	7.5Ω
	DC Load Inductance	2mH

Fig. 8. Voltage Source Inverter showing the 3-Phase Source

3.2.2 Control of DC voltage of the DC link capacitor (v_{dc})

The DC voltage around the capacitor of the VSI must be kept constant. The cause of its variation is the power exchange between the grid and the capacitor. The variations of this voltage must be small in order not to exceed the voltage limits of the semi-conductors and also not to affect the performance of the filter. To ensure the regulation of the dc capacitor voltage, a PI controller is used as illustrated in Fig. 9.

3.2.3 PI controller

The PI controller consist of a proportional term and an integral term. Proportional value determines the reaction to the current error; the

Integral determines the reaction based on the sum of recent errors. The reference currents for the control of active filter are generated according to equation (1). The output of the PI controller at the DC bus voltage of active filter is considered as the current (i_{loss}) in order to meet its losses (Fig. 9).

3.2.4 Voltage source inverter switching

The switching technique employed for the VSI control was the sinusoidal PWM. A PI controller was used to determine the voltage reference of the inverter from the error between the measured current and its reference. This reference voltage was then compared with a triangular carrier signal (with high frequency defining the switching frequency). This is illustrated by Fig. 10. The output of this comparison provided the switching function of the VSI.

3.2.5 The complete model

The simulated system is a three phase balanced and non-balanced voltage system; and the non-linear load used in this work was modeled by a three phase non controlled bridge rectifier. The circuit simulated a typical shunt APF with an AC side IGBT inverter, series inductor, and DC capacitor energization. Two diode rectifiers with a 30 degree phase shift make up the load. The load is changed from 6-pulse to 12-pulse after 10 cycles by connecting the Delta-Y connected rectifier. To create a reference sinusoidal source current that is in phase and has the same RMS

gain as the load current, the SAPF employs a PI control system. The current error between the load current and the reference current is generated by the IGBT Bridge through hysteresis switching. The SAPF was used to inject this current error at the point of common coupling (PCC) in order to match the source current as closely as possible with the reference current. The complete Simulink model of the system is shown in Fig. 11.

3.3 System Simulation Results

In this study MATLAB/SIMULINK is used to implement the designed SAPF under different load conditions. Mainly, there were two simulations; in the first simulation the system had a non-linear load without the SAPF connected, while in the second simulation, the system was connected to the SAPF. The first simulation diagram is as shown in Fig. 12. A three-phase supply feeding a non-linear load with R-L parameters along with 3-phase, 2-level VSI was considered for simulation. The values of simulation parameters are given in Table 2.

The second simulation setup was used to investigate the working of the SAPF; it was connected under different conditions of suddenly connected R-L load of 60Ω, 50mH and unbalanced R-L load of 5Ω, 10Ω, 15Ω on each phase respectively as shown in Fig. 13. The comparator signal (in PI controller) was used to activate the VSI power switching.
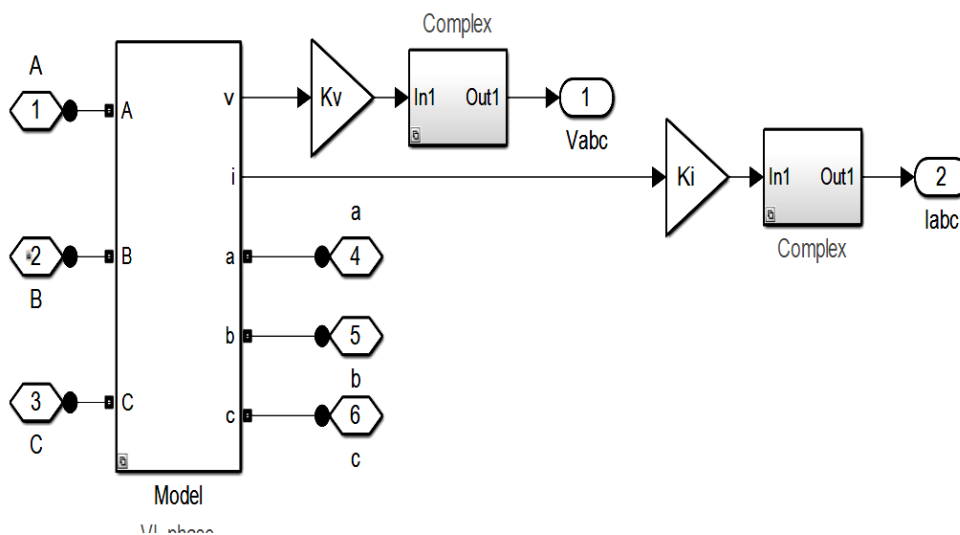

Fig. 9. The PI Controller for the Reference Current generation and Control
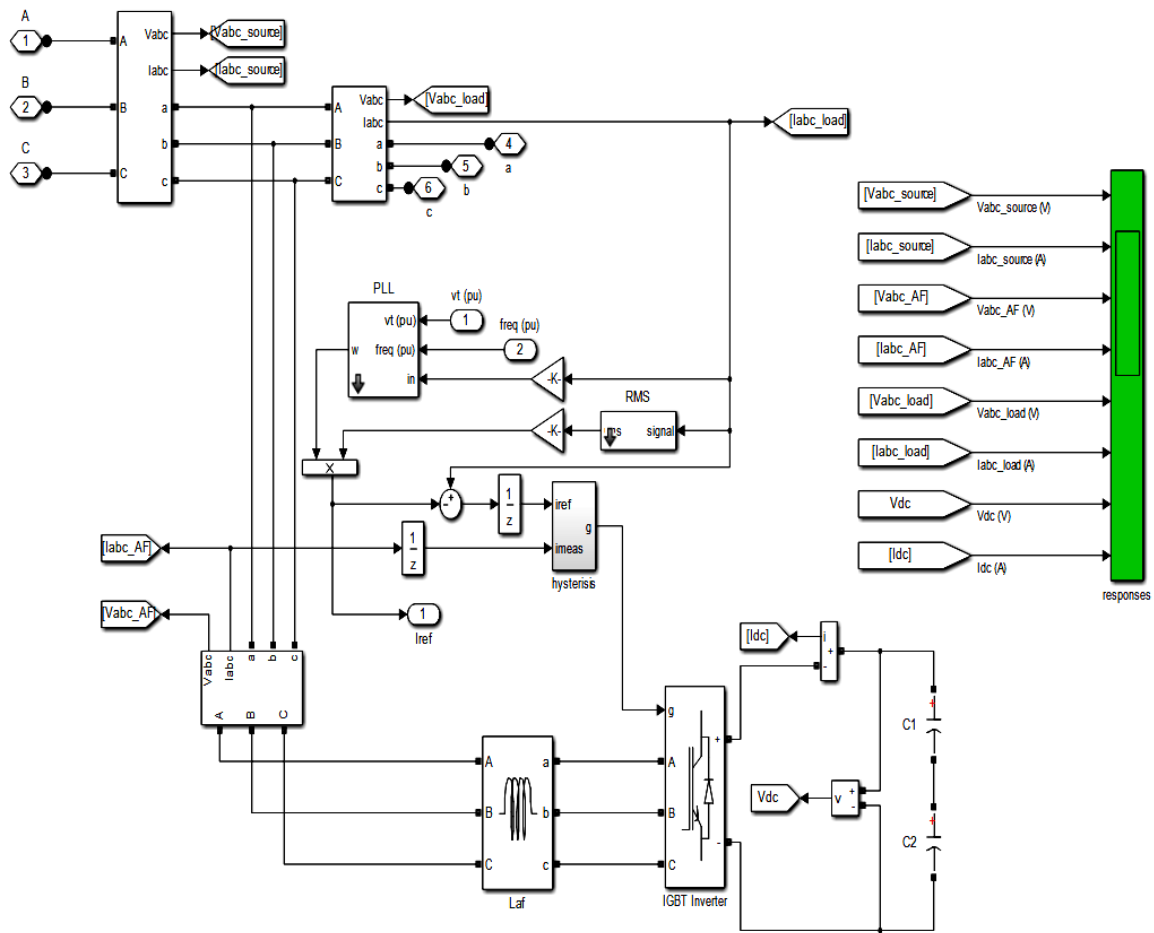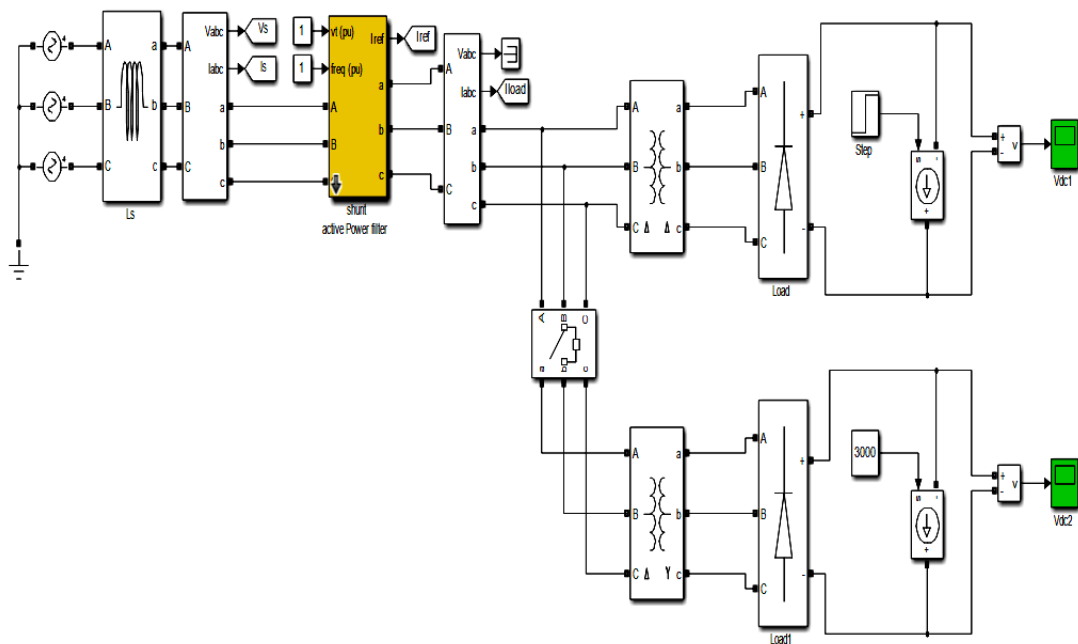
Fig. 10. Voltage source inverter switching

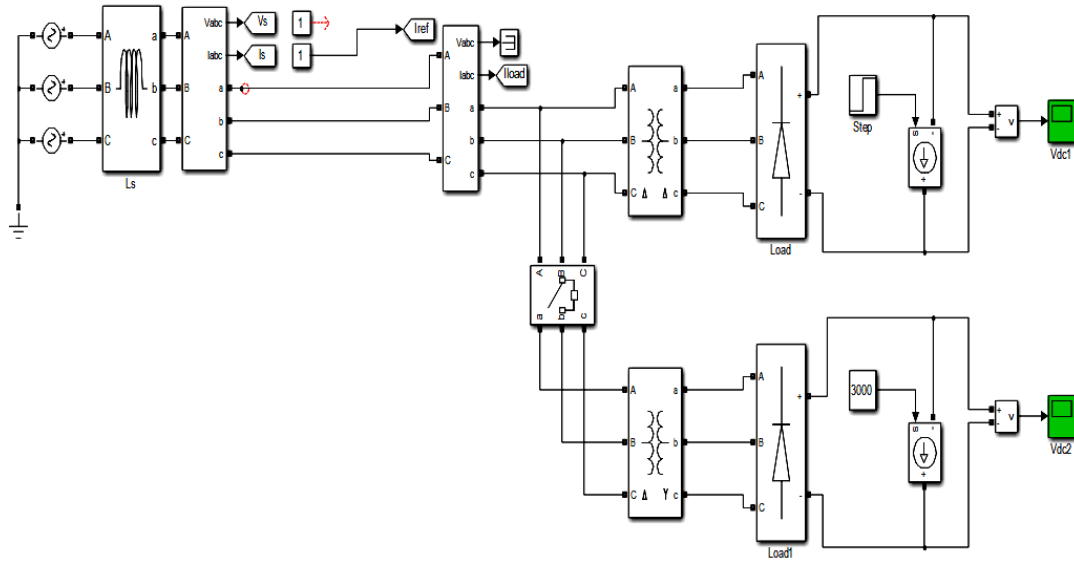**Fig. 11. Complete model of the system**

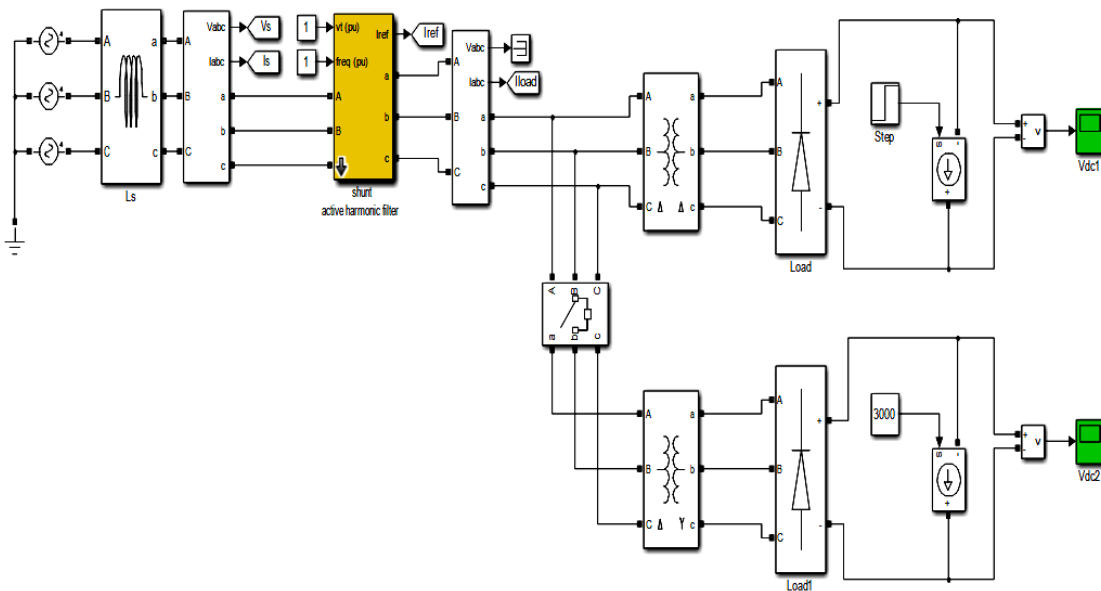**Fig. 12. First Simulation output with a non-linear load without the SAPF connected**

Fig. 13. Second Simulation output with different loads with the SAPF connected

3.4 Performance Analysis

3.4.1 Distorted unbalanced system voltages before application of SAPF

The parameters of the unbalanced system with the three phase distorted voltages are measured and presented. The unbalanced fundamental voltages at 50Hz along with some different amounts of 3rd, 5th, 7th, and 9th harmonics which affects the voltage phases 'a', 'b' and 'c' are recorded and present in Table 3. The total

harmonic distortion (THD) in each phase was calculated using equation (33) as follows:

$$THD_{phase\ A} = \frac{\sqrt{21^2 + 14^2 + 12^2 + 5^2}}{226} = 0.1256$$

$$THD_{phase\ B} = \frac{\sqrt{17.6^2 + 15.5^2 + 12^2 + 7^2}}{240} = 0.1135$$

$$THD_{phase\ C} = \frac{\sqrt{19.5^2 + 12.7^2 + 10^2 + 9^2}}{233} = 0.1120$$

Therefore the THD in the voltage in phase 'a' is 12.6%, while that in phase 'b' is 11.4%, and that in phase 'c' is 11.2%.

19

Table 3. Distorted unbalanced system voltages before application of SAPF

Harmonic Level	Fundamental	3rd	5th	7th	9th	
Frequency (Hz)	50	150	250	350	450	THD%
Phase a (rms)	226	21.0	14.0	12	5	12.6
Phase b (rms)	240	17.6	15.5	12	7	11.4
Phase c (rms)	233	19.5	12.7	10	9	11.2

3.4.2 Filtered unbalanced system voltages after application of SAPF

The three phase grid voltages after the application of SAPF with P-Q control theory are measured and presented. The voltages for the phases 'a', 'b' and 'c' at the fundamental frequency (50Hz), alongside the voltages corresponding to the 3rd, 5th, 7th and 9th harmonic levels are recorded and presented in Table 4. The total harmonic distortion (THD) in each phase is calculated using equation (33) as follows:

$$THD_{phase\ A} = \frac{\sqrt{3^2 + 2.8^2 + 2.6^2 + 2.2^2}}{238} = 0.022$$

$$THD_{phase\ B} = \frac{\sqrt{4.1^2 + 3.5^2 + 2.1^2 + 1.9^2}}{240} = 0.025$$

$$THD_{phase\ B} = \frac{\sqrt{3.9^2 + 3.5^2 + 2.4^2 + 1.2^2}}{239} = 0.025$$

Therefore the THD in the voltage in phase 'a' is 2.2%, while that in phase 'b' is 2.5%, and in phase 'c' is 2.5%.It can now be seen that the phase voltages are approximately balanced, owing to the reactive compensation offered by the P-Q control.

3.4.3 Grid currents before application of SAPF

The three phase load currents in the unbalanced system before harmonic compensation are measured and presented. The currents in the phases 'a', 'b' and 'c' at the fundamental frequency (50Hz), alongside the currents corresponding to the 3rd, 5th, 7th and 9th harmonic levels are recorded and presented in Table 5. The total harmonic distortion (THD) in each phase current is calculated using equation (33) as follows:

$$THD_{I\_phase\ A} = \frac{\sqrt{14.3^2 + 8.5^2 + 3.1^2 + 3.3^2}}{63.5} = 0.272$$

$$THD_{I\_phase\ B} = \frac{\sqrt{10.9^2 + 6.6^2 + 5.1^2 + 4.9^2}}{47.1} = 0.309$$

$$THD_{I\_phase\ B} = \frac{\sqrt{10.9^2 + 9.8^2 + 9.2^2 + 9.1^2}}{63} = 0.310$$

Therefore the THD in the current in phase 'a' is 27.2%, while that in phase 'b' is 30.9%, and that in phase 'c' is 31.0%. It can now be seen that the phase voltages are unbalanced, owing to the effects of harmonic components present in the current signals.

3.4.4 Grid currents after application of SAPF

The three phase load currents in the system after harmonic compensation are measured and presented. The currents in the phases 'a', 'b' and 'c' at the fundamental frequency (50Hz), and the currents corresponding to the 3rd, 5th, 7th and 9th harmonic levels are recorded and presented in Table 6. The total harmonic distortion (THD) in each phase current is calculated using equation (33) as follows:

$$THD_{I\_phase\ A} = \frac{\sqrt{0.8^2 + 0.74^2 + 0.65^2 + 0.46^2}}{62.8} = 0.0215$$

$$THD_{I\_phase\ B} = \frac{\sqrt{0.9^2 + 0.71^2 + 0.61^2 + 0.45^2}}{62.15} = 0.0221$$

$$THD_{I\_phase\ B} = \frac{\sqrt{0.8^2 + 0.7^2 + 0.57^2 + 0.45^2}}{62.65} = 0.0205$$

Therefore the THD in the current in phase 'a' is 2.2%, while that in phase 'b' is 2.2%, and in phase 'c' is 2.1%.

Fig. 14(a) illustrates the distortion in the three-phase grid voltage signals with irregular phase displacements. The THD levels of the signals are between 11.2% and 12.5%. The DC voltage converges perfectly to its reference as shown in Fig. 14(b). The DC voltage of the SAPF demonstrates the PI voltage controller's efficiency in controlling the capacitor voltage. The capacitor voltage clearly follows its defined reference, with fluctuation dependent on power exchange between the grid and the SAPF. The steady-state voltage fluctuation was always less than 0.4% of the reference voltage. The filtered unbalanced system voltages after application of SAPF is shown in Fig. 15.

Table 4. Filtered Unbalanced System Voltages after Application of SAPF

Harmonic Level	Fundamental	3rd	5th	7th	9th	
Frequency (Hz)	50	150	250	350	450	THD%
Phase A (rms)	238	3.0	2.8	2.6	2.2	2.2
Phase B (rms)	240	4.1	3.5	2.1	1.9	2.5
Phase C (rms)	239	3.9	3.5	2.4	1.2	2.5

Table 5. Grid Currents before Application of SAPF

Harmonic Level	Fundamental	3rd	5th	7th	9th	
Frequency (Hz)	50	150	250	350	450	THD%
Phase a (rms)	63.5	14.3	8.5	3.1	3.3	27.2
Phase b (rms)	47.1	10.9	6.6	5.1	4.9	30.9
Phase c (rms)	63.0	10.9	9.8	9.2	9.1	31.0

Table 6. Grid Currents after Application of SAPF

Harmonic Level	Fundamental	3rd	5th	7th	9th	
Frequency (Hz)	50	150	250	350	450	THD%
Phase a (rms)	62.80	0.80	0.74	0.65	0.46	2.2
Phase b (rms)	62.15	0.90	0.71	0.61	0.45	2.2
Phase c (rms)	62.65	0.80	0.70	0.57	0.45	2.1

a) Distorted grid voltages without SAPF   b) DC link simulation with PI controller
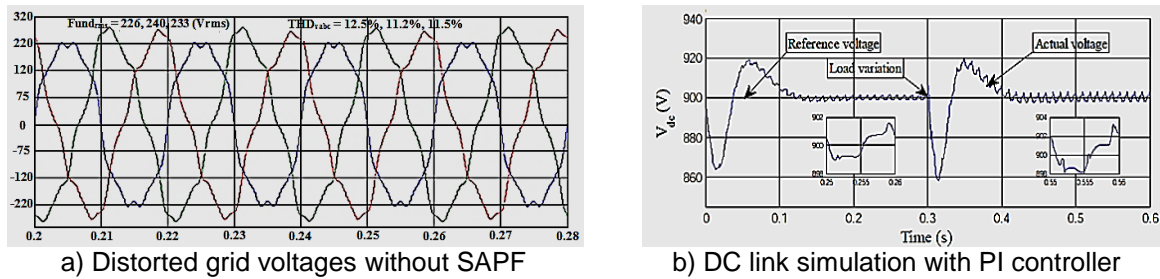
Fig. 14. Distorted grid voltages without SAPF and dc link simulation with PI controller
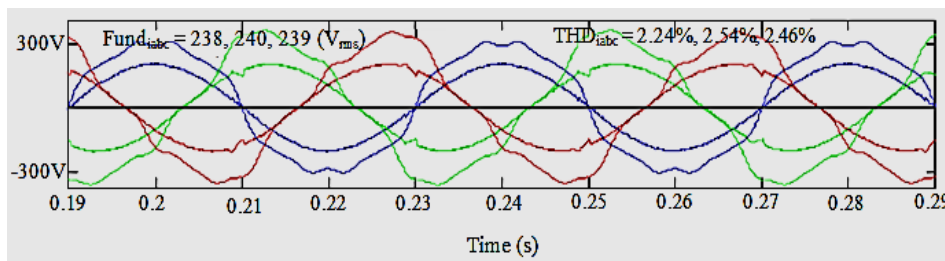

Fig. 15. Filtered unbalanced system voltages after application of SAPF

From Fig. 15, it can be seen that the THD was decreased to values varying between 2.24% for best case; and 2.54% for the worst case, while the use of P-Q Theory-based PI controller in the alpha-beta reference frame has consolidated the performance of the SAPF with the grid voltage waveforms rendered perfectly sinusoidal; and with regular 120˚ phase intervals within one another. Fig. 16(a) shows the grid currents before the application of the filter; with noticeable distortions attributable to the harmonic components present. The THD values range between 27.11% and 31.04%, exceeding the acceptable limits of 5%. Fig. 16(b) illustrates the compensated grid currents after the application of the filter. The currents are characterized by near-perfect sinusoidal wave forms with even phase shifts of 120˚ between phases.
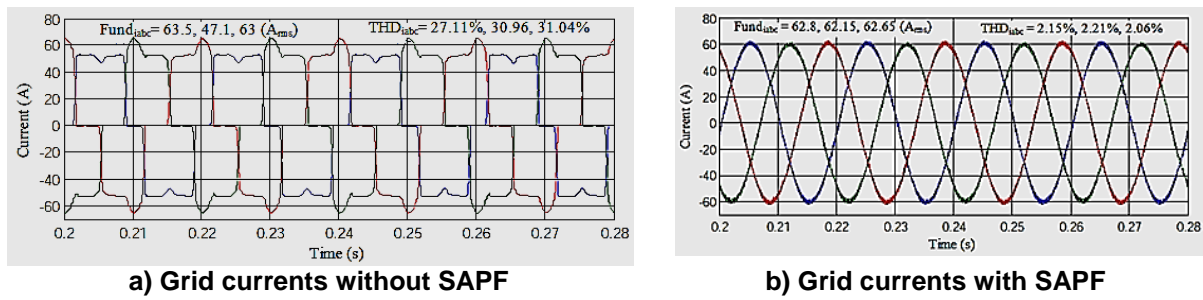
| a) Grid currents without SAPF | b) Grid currents with SAPF |

Fig. 16. Grid currents before and after application of SAPF

4. DISCUSSION

A shunt active power filter was designed and simulated in MATLAB using different load conditions; unbalanced grid voltages and unbalanced grid currents. The use of shunt active filter significantly improved the efficiency of the system harmonic compensation by reducing the overall total harmonic distortion (THD) of the system. The total harmonic distortion (THD) in the unbalanced system voltages before the application of SAPF was found to be 12.6%, 11.4% and 11.2% for phases a, b and c respectively, while after the application of SAPF, the THD was 2.2%, 2.5% and 2.5% for the same respective phase voltages. The grid currents indicated THD of 27.2%, 30.9% and 31% for phase currents a, b and c respectively before application of SAPF, whereas reduced to 2.2%, 2.2% and 2.1% after the application of SAPF.

In electric power systems, lower THD implies lower peak currents, less heating, lower electromagnetic emissions, and less core loss in motors, and lower intermittence in supplied input to grid-sensitive equipment. Because managing harmonics in a power system is considered a joint responsibility involving both end-users and utility owners or operators, harmonic limits are recommended for both voltages and currents. IEEE Standard 519-2014 recommended voltage and current distortion limits of less than 5% of the system total harmonic distortion (THD) for power systems operating on distribution voltage levels between 120V to 69,000V at 50Hz fundamental frequency. It can be seen therefore that the compensated values for both the system voltages and the grid currents are well within the IEEE Standard 519-2014 recommended limits.

These findings is similar to the findings of Agrawal et al. [17] who carried out Performance Analysis of Shunt Active Power Filter Based on Proportional Integral Derivative Acceleration

(PIDA) Controller using P-Q control theory; and obtained an upper harmonic limit of 2.33%.Also, the findings of the current study are similar to the findings of Soomro et al. [18] who carried out design and application of three-phase shunt active power filter (SAPF) using P-Q theory; and obtained a THD limit of 2.54%. However, the findings of this study are not in line with the findings of Agarwal et al. [9], who in their study on the Performance Analysis of Shunt Active Power Filter Based on gravitational search algorithm (GSA) Tuned PI Controller; obtained a THD of 3.13%. The difference in results could be attributed to the difference in the current extraction methods used by both studies, even though both employed Proportional Integral (PI) DC link voltage control. While the current study employed P-Q theory current extraction method, Agarwal et al. [9] used Gravitational Search Algorithm (GSA) current extraction method. Also, findings of this studies differs from the results obtained by Khalid [19] who carried out the performance evaluation of an optimized shunt active power filter using Adaptive Tabu Search (ATS) algorithm and Genetic Algorithm (GA) based on artificial neural networks (ANN); and got a THD of 3.91%. The difference in results could also be attributed to the difference in the reference current extraction methods used in both studies. The findings are also not in line those obtained by Thentral et al. [20], who analyzed the Performance of Shunt Active Filter; and obtained a THD of 3.54%, using Synchronous Reference Frame (SRF) algorithm for the reference current extraction. Evidently, the difference in the methods used for reference current extraction in the two studies account for the dissimilarity in their findings.

Even though findings from the studies of Agarwal et al. [9], Khalid [19] and Thentral et al. [20], were well within the IEEE Standard 519-2014 and 519-1992 recommended limits for system THD, the use of P-Q theory current extraction method with Proportional Integral (PI) DC link voltage Control

have proved to be a better method for the mitigation of Total Harmonic Distortion.

5. CONCLUSION

This study carried out the performance analysis of a Shunt Active Power Filter for suppressing power system harmonics, reactive power compensation and load balancing using PI Controller. The operating principles of the Shunt AF were presented, including the modelling of the system state equations, description of different parts of the model used and the DC link voltage control. The DC bus voltage has been maintained constant equal to the reference voltage by the PI controller. With the combination of different control levels involved, and the non-complex nature of the modelled grid, the choice of the PI Controller is a trade-off between cost and efficacy. The traded efficacy is just a little over 10% compared to over 50% cost differences. Comparative analysis of THD values showed that the system performed well within the stated objectives of harmonic reduction. A comparative analysis of the Root Mean Square (RMS) values and THD of the source voltages and currents of the Load were carried out. The source and load THD is reduced below IEEE standard 519-2014 recommended limits of 5% with the PI controller. After compensation both source and load voltages and currents were in phase with each other implying that the harmonics were eliminated and reactive power was effectively compensated to make power factor close to unity. In addition, the source and load voltages and currents were near-perfect sinusoidal after compensation indicating that power quality has been significantly improved. This system is versatile with applications in thyristor-controlled AC voltage regulators, variable speed drives, electric arc furnaces, and arc welders.

COMPETING INTERESTS

Authors have declared that no competing interests exist.

REFERENCES

1. Demirdelen T. Modelling and Analysis of Multilevel Parallel Hybrid Active Power Filter. M.Sc. Dissertation submitted to the Department of Electrical and Electronic Engineering, Çukurova University Institute of Natural and Applied Sciences, Turkey (Unpublished); 2013.

2. Tan A, Demirdelen T, Inci M, Bayindir KÇ, Tümay M. Analysis of Power Quality Problems of Coreless Induction Melting Furnace with Exact Simulation Model Based on Field Measurements. 4th International Conference on Power Engineering, Energy and Electrical Drives, Istanbul, Turkey; 2013.

3. Demirdelen T, Inci M, Bayindir KÇ, Tümay M. Review of Hybrid Active Power Filter Topologies and Controllers. 4th International Conference on Power Engineering, Energy and Electrical Drives, Istanbul, Turkey; 2013.

4. Wakileh GJ. Power Systems Harmonics: Fundamentals, Analysis and Filter Design. New Jersey: Springer Science & Business Media; 2001.

5. UÇAK O. Design and Implementation of a Voltage Source Converter Based Hybrid Active Power Filter. MSc Thesis submitted to The Graduate School of Natural And Applied Sciences, Middle East Technical University Ankara, Turkey; 2010.
Available: http://www.etd.lib.metu.edu.tr.

6. Chauhan SK, Shah MC, Tiwari RR, Tekwani PN. Analysis, Design and Digital Implementation of a Shunt Active Power Filter with Different Schemes of Reference Current Generation. IET Power Electronics. 2013;7(1):627–639.
DOI: 10.1049/iet-pel.2013.0113.

7. Dugan RC, McGranaghan MF, Santoso S, Beaty HW. Electrical Power System Quality. London: Mcgraw-Hill; 2012:54(68):70-78.

8. Akagi H. Trends in Active Power Line Conditioners. IEEE Transactions on Power Electronics. 1994;9(3):263.

9. Agarwal S, Kumar BS, Palwalia DK. Performance Analysis Of Shunt Active Power Filter Based On GSA Tuned PI Controller. In Proceedings of the International Conference on Information, Communication, Instrumentation and Control (ICICIC), Kagnapur, India; 2017.
DOI: 10.1109/ICOMICON.2017.8279155.

10. Aher TD, Kukade MR, Pathade SD, Gajeshwar SK. Performance Analysis Based On Hybrid Active Power Filter for Three Phase Four Wire System. IOSR Journal of Electrical and Electronics Engineering (IOSR-JEEE). 2017;1(8):42-47.

11. Singh B, Al-Haddad K, Chandra A. A Review of Active Filters for Power Quality

Improvement. IEEE Transactions on Industrial Electronics. 1999;46(5):960–971.

12. Bhattacharya A, Chakraborty C, Bhattacharya S. (2012). Parallel-Connected Shunt Hybrid Active Power Filters Operating At Different Switching Frequencies For Improved Performance. IEEE Transactions on Industrial Electronics. 2012;59(1):4007–4019.
DOI: 10.1109/TIE.2011.2173893.

13. Akagi H, Kanazawa Y, Nabae A. Instantaneous Reactive Power Compensator Comprising Switching Devices without Energy Storage Components. IEEE Transactions on Industrial Applications. 1984;20(3):625-630.

14. Singh B, Singh BN, Chandra A, Al-Haddad K, Pandey A, Kothari DP. A Review of Three-Phase Improved Power Quality AC-DC Converters. IEEE Transactions on Industrial Electronics. 2004;51(1):641–660.
DOI: 10.1109/TIE.2004.825341.

15. Chauhan SK, Shah MC, Tiwari RR, Tekwani PN. Analysis, Design and Digital Implementation of a Shunt Active Power Filter with Different Schemes of Reference Current Generation. IET Power Electronics. 2013;7(1):627–639.
DOI: 10.1049/iet-pel.2013.0113.

16. Balasubramanian R, Palani S. Simulation and Performance Evaluation of Shunt Hybrid Power Filter for Power Quality Improvement Using PQ Theory.

International Journal of Electrical and Computer Engineering. 2016;6(1):2603–2609.
DOI: 10.11591/ijece.v6i6.pp2603-2609.

17. Agarwal S, Gupta VK, Palwalia DK, Somani RK. Performance Analysis of Shunt Active Power Filter Based on PIDA Controller. In the proceedings of the 2nd International Conference on Micro-Electronics and Telecommunication Engineering (ICMETE), Sept. 2018, Ghaziabad, India; 2018.
DOI: 10.1109/ICMETE.2018.00038.

18. Soomro DM, Omran MA, Alswed SK. Design of Shunt Active Power Filter to Mitigate the Harmonics Caused By Nonlinear Loads. ARPN Journal of Engineering and Applied Sciences. 2015;10(19):8774-8782.

19. Khalid S. Performance evaluation of Adaptive Tabu Search and Genetic Algorithm Optimized Shunt Active Power Filter Using Neural Network Control for Aircraft Power Utility of 400 Hz. Journal of Electrical Systems and Information Technology. 2017;1-13.
DOI: 10.1016/j.jesit.2017.04.003.

20. Thentral TMT, Jegatheesan R, Kumar KV. Performance Analysis of Shunt Active Filter with an Adjustable Speed Drive System. Journal of Engineering and Applied Sciences. 2017;12(7):8153-8159.
DOI: 10.36478/jeasci.2017.8153.8159.